ISSN 1674-1056
http://cpb.iphy.ac.cn
http://iopscience.iop.org/cpb
中国物理 B
Chinese Physics
中国物理
Chinese Physics B

Electronic and optical properties of GaN-MoS_2 heterostructure from first-principles calculations

Dahua Ren(任达华), Xingyi Tan(谭兴毅), Teng Zhang(张腾), Yuan Zhang(张源)

Citation: Chin. Phys. B . 2019, 28(8): 086104. **doi:** 10.1088/1674-1056/28/8/086104
Journal homepage: http://cpb.iphy.ac.cn; http://iopscience.iop.org/cpb

What follows is a list of articles you may be interested in

Quantum density functional theory studies of structural, elastic, and opto-electronic properties of $ZMoO_3$(Z=Ba and Sr) under pressure

Saad Tariq, A A Mubarak, Saher Saad, M Imran Jamil, S M Sohail Gilani
Chin. Phys. B . 2019, 28(6): 066101. **doi:** 10.1088/1674-1056/28/6/066101

Effects of Al component content on optoelectronic properties of $Al_xGa_{1-x}N$

Yan-Jun Ji(纪延俊), Jun-Ping Wang(王俊平), You-Wen Liu(刘友文)
Chin. Phys. B . 2018, 27(10): 106102. **doi:** 10.1088/1674-1056/27/10/106102

Bandgap engineering to tune the optical properties of $Be_xMg_{1-x}X$ (X=S, Se, Te) alloys

B Sabir, N A Noor, M Rashid, Fasih Ud Din, Shahid M Ramay, Asif Mahmood
Chin. Phys. B . 2018, 27(1): 016101. **doi:** 10.1088/1674-1056/27/1/016101

Ab-initio investigation of $AGeO_3$ (A=Ca, Sr) compounds via Tran–Blaha-modified Becke–Johnson exchange potential

Rasul Bakhsh Behram, M A Iqbal, Muhammad Rashid, M Atif Sattar, Asif Mahmood, Shahid M Ramay
Chin. Phys. B . 2017, 26(11): 116103. **doi:** 10.1088/1674-1056/26/11/116103

Electronic, optical, and mechanical properties of BN, AlN, and InN with zinc-blende structure under pressure

A R Degheidy, E B Elkenany
Chin. Phys. B . 2017, 26(8): 086103. **doi:** 10.1088/1674-1056/26/8/086103

Electronic and optical properties of GaN–MoS_2 heterostructure from first-principles calculations*

Dahua Ren(任达华)†, Xingyi Tan(谭兴毅), Teng Zhang(张腾), and Yuan Zhang(张源)

School of Information Engineering, Hubei Minzu University, Enshi 445000, *China*

(Received 15 April 2019; revised manuscript received 31 May 2019; published online 9 July 2019)

Heterostructures (HSs) have attracted significant attention because of their interlayer van der Waals interactions. The electronic structures and optical properties of stacked GaN–MoS_2 HSs under strain have been explored in this work using density functional theory. The results indicate that the direct band gap (1.95 eV) of the GaN–MoS_2 HS is lower than the individual band gaps of both the GaN layer (3.48 eV) and the MoS_2 layer (2.03 eV) based on HSE06 hybrid functional calculations. Specifically, the GaN–MoS_2 HS is a typical type-II band HS semiconductor that provides an effective approach to enhance the charge separation efficiency for improved photocatalytic degradation activity and water splitting efficiency. Under tensile or compressive strain, the direct band gap of the GaN–MoS_2 HS undergoes redshifts. Additionally, the GaN–MoS_2 HS maintains its direct band gap semiconductor behavior even when the tensile or compressive strain reaches 5% or −5%. Therefore, the results reported above can be used to expand the application of GaN–MoS_2 HSs to photovoltaic cells and photocatalysts.

Keywords: GaN–MoS_2 heterostructure, electronic structures, optical properties, first-principles calculations

PACS: 61.72.uj, 71.15.Mb, 74.78.Fk **DOI:** 10.1088/1674-1056/28/8/086104

1. Introduction

Stacked van der Waals (vdW) heterostructures (HSs) often lead to new physics and to promising opportunities for the design of unusual electronic devices.[1] Therefore, two-dimensional (2D) vertically stacked vdW HSs have drawn the attention of many researchers because of their tunable band gaps and thicknesses of several atomic layers.[2] For example, MoS_2–ZnO,[3] MoS_2–WSe_2,[4] BP–BN,[5] $MoSe_2$–graphene,[6] and AlGaN–GaN[7] have provided novel material platforms to explore a range of innovative applications, including ultrathin photodetectors,[8] solar cells,[9] and tunneling transistor-based memory devices.[10] However, the application of these 2D materials is enabled by their outstanding physical properties. In addition, the electronic structures of these materials are highly sensitive to both thickness and external strain.[11–15] Miwa *et al.* demonstrated that MoS_2–graphene HSs could be grown epitaxially on a semiconducting silicon carbide substrate under ultrahigh vacuum conditions.[16] In a recent work by He *et al.*, the band gap of the $MoSe_2$–WSe_2 HS was reduced to 1.48 eV, which was lower than the band gaps of the individual WSe_2 (1.60 eV) and $MoSe_2$ (1.50 eV) layers, and the direct or indirect band gaps of HSs have shown redshifts under tensile strains.[17] Overall, strain can be feasibly used to tune the band gaps of these 2D materials.

GaN has recently drawn considerable interest and 2D GaN has been used in optoelectronic applications. Unlike other 2D materials, wurtzite structured bulk GaN is unsuitable for 2D structure formation through exfoliation.[18] Fortunately, 2D GaN has been experimentally synthesized directly via a graphene encapsulation process.[19] Sun *et al.* systematically investigated the electronic properties of a graphene-g-GaN HS based on first-principles calculations and discovered that an increase in the interlayer distance from 2.5 Å to 4.5 Å led to a transition from a p-type to an n-type Schottky contact.[20] Subsequently, the stability properties of 2D GaN have also been confirmed theoretically.[21–23] Sanders *et al.* investigated the electronic and optical properties of both monolayer and bilayer 2D GaN.[24] Accurate band gaps, excitonic properties, and the luminescence energies of 2D GaN under various strains were studied via first-principles calculations based on density functional theory (DFT) and many-body perturbation theory, and it was revealed that the quantum confined Stark effect was amplified by the strong polarization field of the material. With its excellent properties, 2D GaN could be applied in fields including energy-efficient display applications, nonlinear optics, and water purification.[24] In addition, 2D GaN and transition metal dichalcogenides can be combined to provide superior physical properties.

2D MoS_2, a typical direct band gap (1.8 eV) semiconductor, has also received significant attention.[25,26] Monolayer MoS_2 can absorb light in the 510 nm–780 nm range with absorbance of 5%–10%.[26] Therefore, the exploration of the novel structures and excellent properties of GaN–MoS_2 HSs is of great importance. To the best of our knowledge, the electronic and optical properties of GaN–MoS_2 HS have not been

*Project supported by the National Natural Science Foundation of China (Grant No. 11864011), the Hubei Provincial Natural Science Foundation of China (Grant No. 2018CFB390), and the Doctoral Fund Project of Hubei Minzu University, China (Grant No. MY2017B015).

†Corresponding author. E-mail: rdh_perfect@163.com

© 2019 Chinese Physical Society and IOP Publishing Ltd

investigated previously. The study of the structural, electronic, and optical properties of GaN–MoS_2 HSs is very valuable because of the potential applications of these structures in the fields of photovoltaic cells and photocatalysis.

2. Computational methods

All the properties of GaN–MoS_2 HSs were studied using first-principles calculations based on DFT. The generalized gradient approximation of the Perdew–Burke–Ernzerhof functional[27] was adopted and implemented in Vienna *ab initio* simulation package software.[28–31] The projector augmented wave method was used to solve the Kohn–Sham equations.[32] An energy cutoff of 600 eV and Brillouin zone sampling of a K-mesh of $11 \times 11 \times 1$ were set. Additionally, a K-mesh of $15 \times 15 \times 1$ was used for the energy band structure calculations. In the relaxation process, the energy criterion was set at 10^{-5} eV and the residual force was less than 10^{-3} eV/Å. The vacuum layer thickness was more than 20 Å to prevent spurious interactions with the neighboring image structures. The long-range vdW interactions were important in holding the 2D HS together.[33] The vdW-DF2 functional was selected here to describe the long-range electron correlation effects.[34]

In the optical properties calculations, the Fourier transform of the dielectric function was given as[35]

$$\varepsilon_{G,G'}(q,\omega) = \delta_{G,G'}(q,\omega) - \frac{4\pi e^2}{|G+q||G'+q|} X^0_{G,G'}(q,\omega), \quad (1)$$

where q is the Bloch vector, and both G and G' represent reciprocal lattice vectors. The matrix χ_0 was originally derived by Adler.[36] First, the electronic ground state was determined. This meant that the frequency-dependent dielectric matrix could then be derived. After summation over the empty states, the imaginary part was obtained as[36]

$$\varepsilon''_{\alpha\beta}(\omega) = \frac{4\pi^2 e^2}{\Omega} \frac{1}{q} \sum_{c,v,k} 2\omega_k \delta(\varepsilon_{ck} - \varepsilon_{vk} - \omega) \times u_{ck+e_\alpha q} \left| u_{vk} u_{ck+e_\alpha q} \right| u_{vk}, \quad (2)$$

where c and v represent the conduction and valence band states, respectively, e_α describes the unit vectors along three directions, ε_{ck} and ε_{vk} represent the energies of the conduction band and the valence band, respectively, and u_{ck} is the orbital at point k. The dielectric tensor for the real part can be determined based on the Kramers–Kronig formation[36]

$$\varepsilon'_{\alpha\beta}(\omega) = 1 + \frac{2}{\pi} P \int_0^\infty \frac{\varepsilon''_{\alpha\beta}(\omega')\,\omega'}{\omega'^2 - \omega^2 + i\eta} d\omega', \quad (3)$$

where P is the principal value.

3. Results and discussion

The wurtzite GaN structure is cleaved along [0001] to form a planar structure, which was previously predicted to be stable.[19] After optimization, the lattice constants of monolayer GaN and MoS_2 were determined to be 3.18 Å and 3.20 Å, respectively; these values are consistent with previously reported results.[12,24] The structure of the GaN–MoS_2 HS is depicted in Fig. 1. The GaN–MoS_2 HS can be formed with only a small lattice mismatch (0.3%). The lattice parameter of the GaN–MoS_2 HS is 3.19 Å, as calculated using DFT. A supercell (4×4) is then adopted to calculate the properties of the HS.

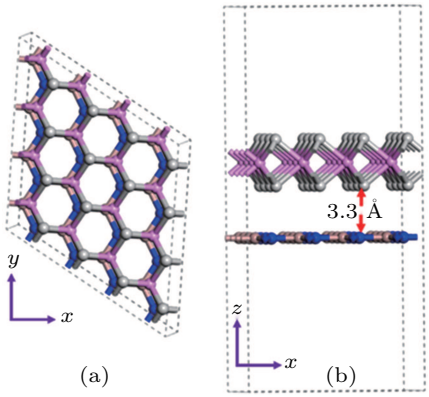


Fig. 1. Structure (4×4 supercells) of GaN–MoS_2 HS from (a) the top view and (b) the side view, where the purple, gray, blue, and brown balls represent the Mo, S, N, and Ga atoms, respectively.

To assess the vdW interactions between the GaN and MoS_2 layers, the distance D between the Ga and S atoms and the binding energy ΔE are calculated for the GaN–MoS_2 HS as follows:

$$\Delta E = E_{\mathrm{HS}} - E_{\mathrm{MoS_2}} - E_{\mathrm{GaN}}, \quad (4)$$

where ΔE represents the binding energy of the GaN–MoS_2 HS. E_{HS}, $E_{\mathrm{MoS_2}}$, and E_{GaN} represent the total energies of the HS, the MoS_2 monolayer, and the GaN monolayer, respectively. It is indicated that the binding energy is 0.20 eV based on physical adsorption, and the distance D between the Ga and S atoms is approximately 3.30 Å, which means that no bond is formed between the Ga and S atoms. This confirms that vdW interactions occur between the two layers.

Next, the band structure of the GaN–MoS_2 HS is derived, as shown in Fig. 2. Both the valence band maximum (VBM) and the conduction band minimum (CBM) of the GaN–MoS_2 HS remain at the K point, as shown in Fig. 2(b). The band gap of the GaN–MoS_2 HS is 1.95 eV, while that of monolayer GaN is 3.48 eV and that of monolayer MoS_2 is 2.03 eV, based on HSE06 hybrid functional calculations. It is thus demonstrated that the GaN–MoS_2 HS is a typical type-II band semiconductor, as illustrated in Fig. 2(a). In the type-II band alignment, the positions of the valence and conduction bands of the GaN semiconductor are higher than the corresponding bands of the MoS_2 semiconductor. In addition, the steps in the conduction

and valence bands are oriented in the same direction. Importantly, the difference in the chemical potential between semiconductor GaN and MoS_2 causes band bending at the junction interface. This band bending induces a built-in field that drives the photogenerated electrons and holes to move in opposite directions, which leads to spatial separation of the electrons and holes on the different sides of the heterojunction.[37] Type-II HSs are of particular interest because of this spatial separation of the electrons and holes following photoexcitation, which is a highly desirable property for photovoltaic applications.[38] Therefore, the type-II band behavior of the GaN–MoS_2 HS could be applicable in the photovoltaic and photocatalytic fields.

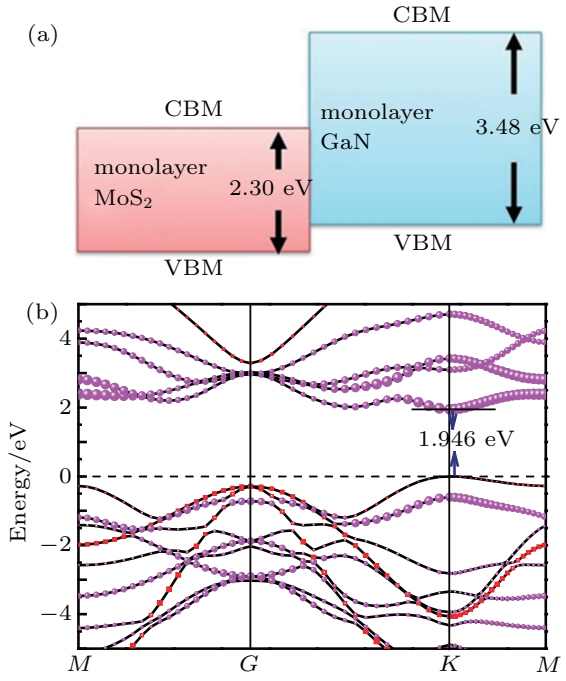


Fig. 2. (a) Schematic diagram of a typical type-II band and (b) band structure of the GaN–MoS_2 HS, where the purple and red balls represent the MoS_2 and GaN contributions, respectively.

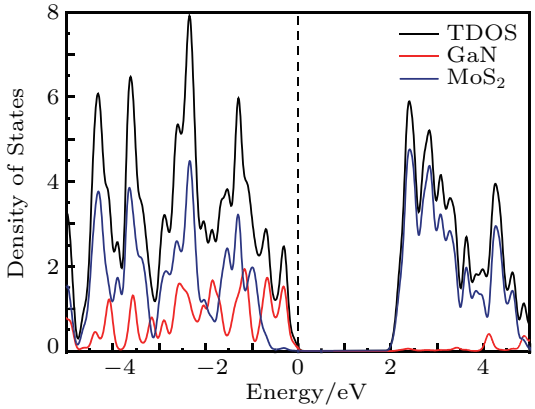


Fig. 3. Total density of states of GaN, MoS_2, and the GaN–MoS_2 HS.

To gain an insight into the electronic properties of the GaN–MoS_2 HS, the total density of states and the projected density of states are presented in Fig. 3. The red and blue lines represent the DOSs of GaN and MoS_2 in the GaN–MoS_2 HS, respectively. The figure clearly shows that the VBM and the CBM are confined within the GaN and MoS_2 layers, respectively.

For further clarification of the interactions, the electronic band structure of the GaN–MoS_2 HS is calculated under various biaxial strains. Strain is known to be one of most effective means to tailor the properties of 2D materials.[11–13,17] Yu *et al.* calculated the electronic properties of $RbGeI_3$ under strains ranging from −6% to 6% and found that the band gap of the material decreased monotonically.[11] In Fig. 4, the lattice parameters with strains of −5.0% to +5.0% have been added to the structure of the GaN–MoS_2 HS and the band gap properties of the GaN–MoS_2 HS as it varies from compressed to stretched have been investigated. First, the strain may not be transferred entirely from the GaN layer to the MoS_2 layer. Second, to avoid the symmetry of the HS being destroyed, the use of biaxial strain of less than 5% is considered. Both stretching and compression can lead to a reduction of the band gap of the GaN–MoS_2 HS. The calculated band gap shifts with respect to the strain and the band gap are significantly reduced under application of biaxial tensile or compressive strain at 2.0%. The rate of reduction of the direct band gap of the GaN–MoS_2 HS under tensile strain is found to be much higher than that under compressive strain. This is the reason why the VBM at the *K* point is predominantly contributed by the N p_z and Ga p_z, d_{z2}, and d_{yz} orbitals, while the CBM at the *K* point contains a proportion of the metal S p_x and Mo d_{z2} and d_{yz} orbitals. Obviously, the tensile strain results in in-plane expansion of the lattice because of the reduction in the overlap of the metal Ga d orbitals and Mo d orbitals. As a result, the rate of change in the direct band gap of the GaN–MoS_2 HS induced by strain at the *K* point is relatively slow. As indicated by the calculated band structures, the direct band gap is reduced by strain because of the contributions from the upshifted CBM at the *K* point and the downshifted VBM at the *K* point. In particular, the direct band gap peak intensity decreases monotonically under the application of strain, and the +5.0% and −5.0% strains ensure that the stretched and compressed GaN–MoS_2 HSs remain semiconductors. These results agree well with those reported for the WSe_2/$MoSe_2$ HS.[17]

The imaginary part of the dielectric constant ε_2 for the GaN–MoS_2 HS from -5% to 5% strain is then calculated, as shown in Fig. 5. The imaginary part of the dielectric constant can represent the absorption coefficient and the first absorption peak is located at 3.30 eV, which is in the ultraviolet light range. The optical band gap is 1.89 eV, which agrees well with the calculated electronic band gap. It is clearly shown that the optical band gap of the GaN–MoS_2 HS suffers from redshifts under tensile and compressive strain. When the tensile and compressive strain is increased, the absorption intensity is

also enhanced. This means that GaN–MoS_2 HS will be suitable for application to photovoltaic cells and photodetectors in the future.

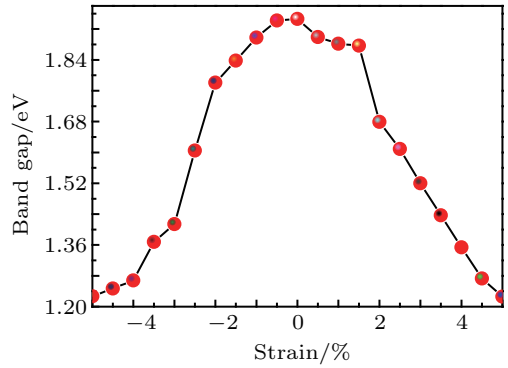


Fig. 4. Band gap of the GaN–MoS_2 HS under various biaxial strains.

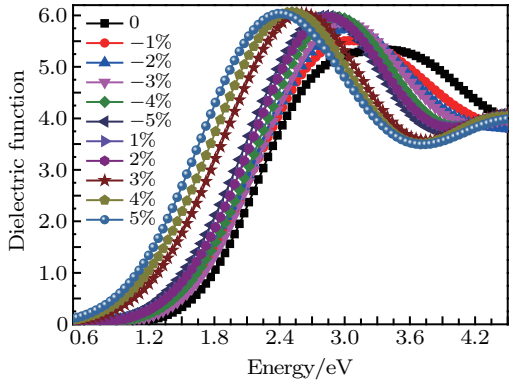


Fig. 5. Imaginary dielectric function of the GaN–MoS_2 HS with strains ranging from −5% to 5%.

4. Conclusion

In summary, the electronic and optical properties of the GaN–MoS_2 HS have been determined from first-principles calculations. The lattice parameter of the GaN–MoS_2 HS is 3.19 Å and the structure of this HS is stable. The GaN–MoS_2 HS is found to be a typical type-II band structure semiconductor. The application of tensile or compressive strain leads to a reduction of the direct band gap of the GaN–MoS_2 HS. These results can offer insights into the interactions between the stacked GaN and MoS_2 monolayers in the GaN–MoS_2 HS and will help to guide the design of future applications of these HSs in solar cells and photocatalysts.

References

[1] Geim A and Grigorieva I 2013 *Nature* **499** 419
[2] Chhowalla M, Liu Z and Zhang H 2015 *Chem. Soc. Rev.* **44** 2584
[3] Selvaraj R, Kalimuthu K R and Kalimuthu V 2019 *Mater. Lett.* **245** 183
[4] Fang H, Battaglia C, Carraro C, Nemsak S, Ozdol B, Kang J S, Bechtel H A, Desai S B, Kronast F and Unal A A 2014 *Proc. Natl. Acad. Sci. USA* **111** 6198
[5] Zhang P, Wang J and Duan X M 2016 *Chin. Phys. B* **25** 037302
[6] Zhang X W, He D W, He J Q, Zhao S Q, Hao S C, Wang Y S and Yi L X 2017 *Chin. Phys. B* **26** 097202
[7] Hou M C, Xie G and Sheng K 2019 *Chin. Phys. B* **28** 037302
[8] Massicotte M, Schmidt P, Vialla F, Schädler K G, Reserbat Plantey A, Watanabe K, Taniguchi T, Tielrooij K J and Koppens F H L 2016 *Nat. Nanotechnol.* **11** 42
[9] Lee C H, Lee G H, van der Zande A M, Chen W, Li Y, Han M, Cui X, Arefe G, Nuckolls C, Heinz T F, Guo J, Hone J and Kim P 2014 *Nat. Nanotechnol.* **9** 676
[10] Britnell L, Gorbachev R V, Jalil R, Belle B D, Schedin F, Mishchenko A, Georgiou T, Katsnelson M I, Eaves L, Morozov S V, Peres N M R, Leist J, Geim A K, Novoselov K S and Ponomarenko L A 2012 *Science* **335** 947
[11] Yu Z L, Ma Q R, Liu B, Zhao Y Q, Wang L Z, Zhou H and Cai M Q 2017 *J. Phys. D: Apll. Phys.* **50** 465101
[12] Wu L J, Zhao Y Q, Chen C W, Wang L Z, Liu B and Cai M Q 2016 *Chin. Phys. B* **25** 107202
[13] Zhao Y Q, Ma Q R, Liu B, Yu Z L, Yang J L and Cai M Q 2018 *Nanoscale* **10** 8677
[14] Wang H, Yuan H, Sae S H, Li Y and Cui Y 2015 *Chem. Soc. Rev.* **44** 2664
[15] Rodin A S, Carvalho A, Castro Neto A H 2014 *Phys. Rev. Lett.* **112** 176801
[16] Miwa J A, Dendzik M, Grønborg S S, Bianchi M, Lauritsen J V, Hofmann P and Ulstrup S 2015 *ACS Nano* **9** 6502
[17] He Y M, Yang Y, Zhang Z H, Gong Y J, Zhou W, Hu Z L, Ye G L, Zhang X, Bianco E, Lei S D, Jin Z H, Zou X L, Yang Y C, Zhang Y, Xie E Q, Lou J, Yakobson B, Vajtai R, Li B and Ajayan P 2016 *Nano Lett.* **16** 3314
[18] Dingle R, Sell D D, Stokowski S E and Ilegems M 1971 *Phys. Rev. B* **4** 1211
[19] Al Balushi Z Y, Wang K, Ghosh R K, ViláR A, Eichfeld S M, Caldwell J D, Qin X, Lin Y C, DeSario P A, Stone G, Subramanian S, Paul D F, Wallace R M, Datta S, Redwing J M and Robinson J A 2016 *Nat. Mater.* **15** 1166
[20] Sun M L, Chou J P, Ren Q Q, Zhao Y M, Yu J and Tang W C 2017 *Appl. Phys. Lett.* **110** 173105
[21] Prete M S, Mosca Conte A, Gori P, Bechstedt F and Pulci O 2017 *Appl. Phys. Lett.* **110** 012103
[22] Lucking M C, Xie W Y, Choe D H, West D, Lu T M and Zhang S B 2018 *Phys. Rev. Lett.* **120** 086101
[23] Zhang H, Meng F S and Wu Y B 2017 *Solid State Commun.* **250** 18
[24] Sanders N, Bayerl D, Shi G, Mengle K A and Kioupakis E 2017 *Nano Lett.* **17** 7345
[25] Sundaram R S, Engel M, Lombardo A, Krupke R, Ferrari A C, Avouris P and Steiner M 2013 *Nano Lett.* **13** 1416
[26] Bernardi M, Palummo M and Grossman J C 2013 *Nano Lett.* **13** 3664
[27] Perdew J P, Burke J P and Ernzerhof M 1996 *Phys. Rev. Lett.* **77** 3865
[28] Kresse G and Hafner J 1993 *Phys. Rev. B* **47** 558
[29] Kresse G and Furthmuller J 1996 *Phys. Rev. B* **54** 11169
[30] Kresse G and Furthmuller J 1996 *Comput. Mater. Sci.* **6** 15
[31] Kohn W and Sham L 1965 *Phys. Rev.* **140** A1133
[32] Blochl P E 1994 *Phys. Rev. B* **50** 17953
[33] Tsoi S, Dev P, Friedman A L, Stine R, Robinson J R, Reinecke T L and Sheehan P E 2014 *ACS Nano* **8** 12410
[34] Lee L, Murray E D, Kong L, Lundqvist B I and Langreth D C 2010 *Phys. Rev. B* **82** 081101
[35] Gajdoš M, Hummer K, Kresse G, Furthmüller J and Bechstedt F 2006 *Phys. Rev. B* **73** 045112
[36] Adler S L 1962 *Phys. Rev.* **126** 413
[37] Wang Y J, Wang Q S, Zhan X Y, Wang F M, Safdar M and He J 2013 *Nanoscale* **5** 8326
[38] Lo S S, Mirkovic T, Chuang C H, Burda C and Scholes G D 2011 *Adv. Mater.* **23** 180